Available online at www.sciencedirect.com
ScienceDirect
Journal of Sound and Vibration 303 (2007) 264–276
JOURNAL OF SOUND AND VIBRATION
www.elsevier.com/locate/jsvi

Vibrational power flow analysis of a submerged viscoelastic cylindrical shell with wave propagation approach

J. Yan[a,*], F.Ch. Li[a], T.Y. Li[b]

[a]Engineering College, Guangdong Ocean University, Zhanjiang 524088, PR China
[b]Department of Naval Architecture and Ocean Engineering, Huazhong University of Science and Technology, Wuhan 430074, PR China

Received 19 January 2006; received in revised form 21 November 2006; accepted 19 January 2007
Available online 6 March 2007

Abstract

The vibrational power flow in a submerged infinite unconstrained viscoelastic cylindrical shell using wave propagation approach is presented. The harmonic motion of the shell and the pressure field in the fluid is described by Flügge shell theory and Helmholtz equation, respectively. The damping characteristics are considered by complex modulus method. Vibrational power flow inputting into the coupled system and propagating along the shell axial direction are both studied. The numerical results indicate input power flow varies with driving frequency and circumferential mode order, and the viscoelastic damping layer will restrict the exciting force inputting power flow into the shell especially for a thicker damping layer and a higher circumferential mode order. Cut-off frequencies do not exist in viscoelastic shell so that the exciting force can input power flow into the shell at any frequency and for any circumferential mode order. Relative to the nearly linear attenuation form of propagation power flow in elastic shell, propagation power flow in viscoelastic shell is exhibited in exponential attenuation form. Viscoelastic layer will have a good damping effect especially at middle or high frequencies. The conclusion may be valuable to the application of viscoelastic damping material on noise and vibration control of submarines and underwater pipes.

1. Introduction

The problem of controlling the noise and vibration of mechanical structures is very important. An effective way to solve the problem is to use the technique of surface damping treatment. When exposed to vibrations, the high polymeric molecular properties exhibited by viscoelastic materials enhance the system damping, thereby realizing considerable dissipation of vibration energy. Viscoelastic coating is usually used in two ways: constrained and unconstrained layer configuration. In unconstrained layer damping, a viscoelastic damping layer is fixed to an elastic base structure, so that energy dissipation occurs in extension. In constrained layer damping, an additional elastic layer (which has an elastic modulus much higher than that of the damping layer) is placed on the damping layer so that energy dissipation occurs in shearing. Vast numerations indicated that energy dissipation in extension is much less than that in shearing, so the damping capacity of constrained layer is better than that of unconstrained layer. However, since the constrained layer will add considerable

*Corresponding author. Tel.: +86 13434662436.
E-mail address: d3219yan@tom.com (J. Yan).

0022-460X/$ - see front matter © 2007 Elsevier Ltd. All rights reserved.
doi:10.1016/j.jsv.2007.01.014

Nomenclature

c_f sound velocity in fluid
d the distance from midsurface radius to viscoelastic shell interface
E_1, E_2 Young's modulus of elastic material or viscoelastic material
f vibratory frequency
F applied harmonic pressure
FL fluid loading
h_1, h_2 thickness of elastic layer or viscoelastic layer
$H_n^{(2)}$ the second kind of Hankel function of order n
k_{ns}, k_0, k_s^r axial wavenumber, free wavenumber or radial wavenumber
n circumferential modal number
$N(x)$, $T(x)$, $S(x)$, $M(x)$ axial force, torsional shear force, transverse shear force or bending moment of the shell
p_f acoustic pressure
P_{input} input power flow
P'_{input} non-dimensional input power flow
$P_{N(x)}$, $P_{T(x)}$, $P_{S(x)}$, $P_{M(x)}$ power flow carried by, axial force, torsional shear force, transverse shear force or bending moment of x cross-section
$P'_{N(x)}$, $P'_{T(x)}$, $P'_{S(x)}$, $P'_{M(x)}$ $P_{N(x)}/P_{\text{shell}(x)}$, $P_{T(x)}/P_{\text{shell}(x)}$, $P_{S(x)}/P_{\text{shell}(x)}$ or $P_{M(x)}/P_{\text{shell}(x)}$
P_r radial force acting on the shell wall
$P_{\text{shell}(x)}$ total power flow of x cross-section
$P'_{\text{shell}(x)}$ $P_{\text{shell}(x)}/(0.5\,P_{\text{input}})$
R shell midsurface radius
s a particular branch of the dispersion curves
u, v, w, $\partial w(x)/\partial x$ shell displacements and slope
$\tilde{U}_{ns}$, $\tilde{V}_{ns}$, $\tilde{W}_{ns}$ shell spectral displacements
x, r, θ cylindrical coordinate
λ non-dimension axial wavenumber
ω circular frequency
δ Dirac delta function
μ_1, μ_2 Poisson's ratio of elastic material or viscoelastic material
η_1, η_2 loss factor of elastic material or viscoelastic material
ρ_1, ρ_2 density of elastic material or viscoelastic material
Ω, Ω_1 non-dimension frequency of elastic shell or viscoelastic shell
∇^2 Laplace operator

Superscripts

$*$ complex conjugate
$()'$ $R\partial(\,)/\partial x$
$()^\circ$ $\partial(\,)/\partial\theta$

mass to the system while the construction process of unconstrained layer is rather simple, unconstrained damping layer is still preferred in many practical situations.

The vibration analysis of a cylindrical shell with a free-layer damping treatment was first conducted by Kagawa and Krokstad [1]. They presented five principal modes (axisymmetrical and axially unaxisymmetrical) in a two-layered shell by introducing damping. The relevant loss factors for pure torsional, radial, longitudinal, circumferential and flexural modes were derived for an infinitely long layered shell. Unfortunately, the derived expressions for the loss factors were based on crude assumptions. The authors were unable to identify the real damping mechanism, which in fact is due to extensional strains in the damping treatment in both longitudinal and circumferential directions. Markuš [2] used classical thin shell theory to study the damping properties of cylindrical shell of finite length, coated on the inside or outside, or on both sides. He called these two-layered damped shells as "Oberst shell". Markuš [3] further analyzed the above problem precisely, and also derived the control differential equation with classical thin shell theory. In both articles, the author adopted the concept of "damped normal mode" [4] and analyzed the non-coupling torsional mode and the coupling longitudinal-radial mode. He pointed out that mechanical dissipation strongly depended on the ratio of thickness to radius (even in axisymmetric modes). Iyer [5] analyzed the forced vibration problem and presented a method to solve forced vibration equations set. The mode response at arbitrary frequency and the influence of the damping layer for different numeric results were also calculated and discussed. Naiyar and Asnani [6] considered extensional deformation, shear deformation and high-order inertia term on the base of classical theory, and calculated the loss factors of the coupling longitudinal-radial

mode and the non-coupling torsional mode with linear elastic-viscoelastic theory. He also pointed out that it would make mistake to calculate loss factors with classical thin shell theory.

Compared with full coverage, partial coverage was investigated to a less degree [7–9]. Besides, location and shape optimization of unconstrained viscoelastic layers for a given weight material have been examined in the literatures [10,11].

The concept of vibrational power flow is very valuable in the analysis of noise and vibration of a shell. Fuller [12] investigated the forced input mobility of an infinite elastic circular cylindrical shell filled with fluid. Xu and Zhang [13] investigated the vibrational power flow input from an external force and the transmission along the shell axial direction by different internal forces of the shell wall. The results showed that the input power flow and the power flow transmission depend mainly upon the characteristics of the free propagating waves in this coupled system. Sorokin [14] formulated an energy flow through arbitrary cross-section of an infinitely long shell at each circumferential mode number. An inspection into the energy redistribution between several transmission paths in a near field and the influence of excitation conditions on steady fluctuations of the overall energy flow in a far field was also performed. The authors [15] also studied the characteristics of the vibrational power flow propagation in an infinite submerged periodic ring-stiffened cylindrical shell.

Although both vibrational power flow and viscoelastic damping layer concerning circular cylindrical shell structure have been studied by numerous scholars, literatures about the characteristics of vibrational power flow in submerged viscoelastic damping cylindrical shell are rarely found. In this paper, vibrational power flow in a submerged infinite unconstrained viscoelastic cylindrical shell excited by a radial harmonic force is investigated with wave propagation approach which was discussed in literature [16]. The harmonic motion of the shell and the pressure field in the fluid is described by Flügge shell theory and Helmholtz equation, respectively. The damping characteristics are considered by complex modulus method. Vibrational power flow inputting into the coupled system and propagating along the shell axial direction are both studied. Numerical computations are implemented and the influences of frequency, circumferential mode order as well as damping material on the results are discussed, respectively.

This paper is organized in five sections. In Section 1, a brief introduction is given. In Section 2, the motion equation of the coupled system is set up and the response to convected harmonic pressure is deduced. In Section 3, input power into the coupled system and propagation power along the shell axial direction are obtained. Numerical computations and relevant results discussion are carried through subsequently in Section 4, and Section 5 gives a brief summary of the conclusions.

2. The response of the coupled system to convected harmonic pressure

An infinite submerged cylindrical shell coated with unconstrained viscoelastic layer is considered. The coordinate system and circumferential modal shapes are shown in Fig. 1. It is assumed the vibrations are small and linear, which is appropriate in most vibroacoustic applications. It is also assumed that each layer of the studied laminated shell structures is isotropic and homogeneous. Finally, if not defined directly in the text, notations used may be found in Nomenclature.

The classical complex modulus method [2] is used to study the damping characteristics of structures. Considering the coupling effect of fluid field and the radial exciting force, the wave motions in the shell wall can be described by Flügge shell equations [9]

$$\left[A_1u'' + \frac{1}{2}(AF_1 - AF_{1r} + BT_1 - BT_{1r})u^{\circ\circ} - \frac{R^2m}{D}\frac{\partial^2 u}{\partial t^2}\right] + \left[\frac{1}{2}(A_1 + A_{1r}) - \frac{1}{4}D_{1r}\right]v'^{\circ} + \left[A_{1r}w' - B_1w''' + BDw'^{\circ\circ}\right] = 0, \tag{1a}$$

$$\left[\frac{1}{2}(A_1 + A_{1r}) - \frac{1}{4}D_{1r}\right]u'^{\circ} + \left[A_1v^{\circ\circ} + AQv'' - \frac{R^2m}{D}\frac{\partial^2 u}{\partial t^2}\right] + \left[A_1w^{\circ} - \frac{1}{2}(3B_1 - B_{1r})w''^{\circ} + \frac{1}{4}(AP_1 - AP_{1r})w''^{\circ}\right] = 0, \tag{1b}$$

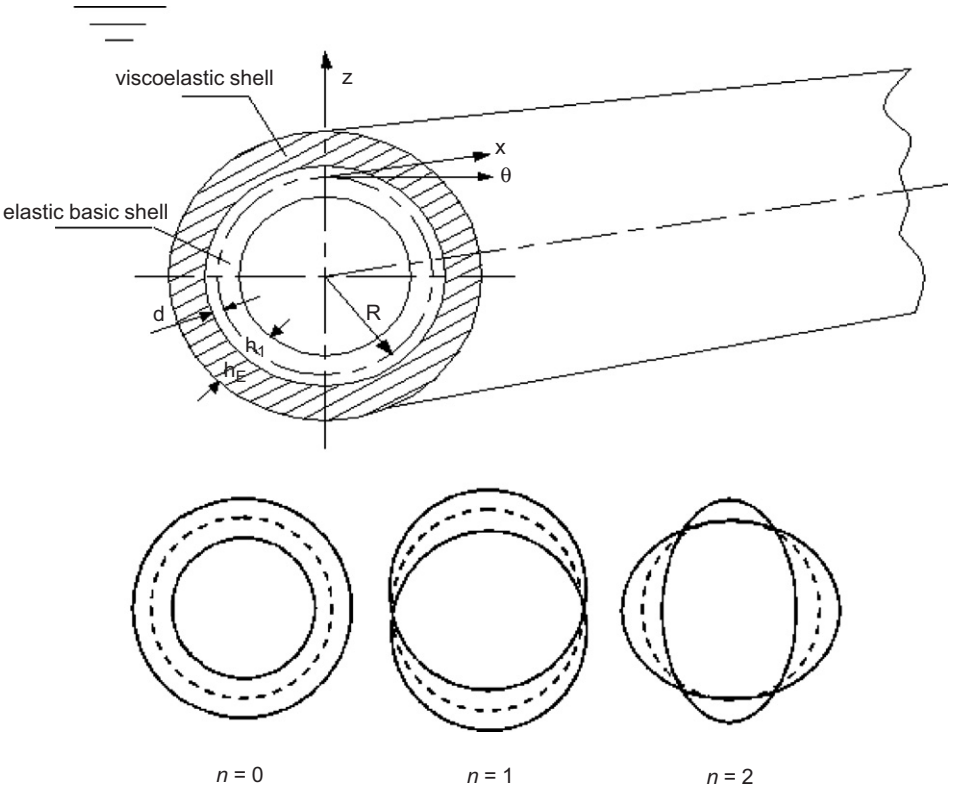

Fig. 1. Coordinate system and circumferential modal shapes.

$$\begin{aligned}&\left[A_{1r}u' - B_1u''' + BDu'^{\circ\circ}\right] + \left[A_1v^{\circ} - \frac{1}{2}(3B_1 - B_{1r})v''^{\circ} + \frac{1}{4}(AP_1 - AP_{1r})v''^{\circ}\right]\\ &+ \left\{(B_1 - \frac{1}{4}AP_1)w'''' + D_{1r}w'' + \left[BD + \frac{1}{2}(3B_1 + B_{1r}) - \frac{1}{4}(AP_1 - AP_{1r})\right]w''^{\circ\circ}\right.\\ &+ 2(-A_1 + AF_1 + BT_1)w^{\circ\circ} + (-A_1 + AF_1 + BT_1)w^{\circ\circ\circ\circ} + (AF_1 + BT_1)w\\ &\left.+ \frac{R^2m}{D}\frac{\partial^2u}{\partial t^2}\right\} = P_rR^2,\end{aligned} \tag{1c}$$

where u, v and w are the displacements of the shell in the direction of the x-, r- and θ-axes, respectively. Other parameters are given in Appendix A.

The shell is excited by a harmonic line force F, acting on $x = 0$, expressed as

$$F(\theta, t) = F_0\ \cos(n\theta)\delta(0)\exp(\mathrm{i}\omega t). \tag{2}$$

The normal mode shapes assumed for the displacement of the shell wall, associated with a branch axial wave number k_{ns}, can be expressed as the form of wave propagation

$$\begin{cases} u = \sum_{n=0}^{\infty}\sum_{s=1}^{\infty} U_{ns}\ \cos(n\theta)\exp(\mathrm{i}\omega t - \mathrm{i}k_{ns}x),\\ v = \sum_{n=0}^{\infty}\sum_{s=1}^{\infty} V_{ns}\ \sin(n\theta)\exp(\mathrm{i}\omega t - \mathrm{i}k_{ns}x),\\ w = \sum_{n=0}^{\infty}\sum_{s=1}^{\infty} W_{ns}\ \cos(n\theta)\exp(\mathrm{i}\omega t - \mathrm{i}k_{ns}x),\end{cases} \tag{3}$$

where subscript s denotes a particular branch of the dispersion curves.

The acoustic wave equation for the fluid satisfies the Helmholtz equation [17] in cylindrical coordinates as

$$\nabla^2 p_f + k_0^2 p_f = 0, \tag{4}$$

where $k_0 = \omega/c_f$.

To ensure the fluid remains in contact with the shell wall, the fluid radial displacement and the shell radial displacement must be equal at the interface of the shell outer wall and the fluid. The coupling condition is $w_{\text{fluid}} = w_{\text{shell}}$ at $r = R$.

Taking the Fourier transform of Eqs. (1) and (4) and applying the coupling condition, the following equations are obtained:

$$\begin{bmatrix} L_{11} & L_{12} & L_{13} \\ L_{21} & L_{22} & L_{23} \\ L_{31} & L_{32} & L_{33} \end{bmatrix} \begin{bmatrix} \tilde{U}_{ns} \\ \tilde{V}_{ns} \\ \tilde{W}_{ns} \end{bmatrix} = \begin{bmatrix} 0 \\ 0 \\ X_{pl} \end{bmatrix}, \tag{5}$$

where

$$L_{11} = -\lambda^2 - \frac{1}{2}\left(\frac{AF_1 - AF_{1r}}{A_1} + \frac{BT_1 - BT_{1r}}{2A_1}\right)n^2 + \Omega_1^2,$$

$$L_{12} = L_{21} = -\mathrm{i}\lambda n\left(\frac{A_1 + A_{1r}}{2A_1} - \frac{D_{1r}}{4A_1}\right),$$

$$L_{13} = L_{31} = -\mathrm{i}\frac{B_1}{A_1}\lambda^3 - \mathrm{i}\frac{(A_{1r} - BD \times n^2)}{A_1}\lambda,$$

$$L_{22} = \frac{AQ}{A_1}\lambda^2 + n^2 - \Omega_1^2,$$

$$L_{23} = L_{32} = -\frac{1}{A_1}\left(\frac{AP_1 - AP_{1r}}{4} - \frac{3B_1 - B_{1r}}{2}\right)n\lambda^2 + n,$$

$$L_{33} = \frac{1}{A_1}\left(B_1 - \frac{AP_1}{4R^3}\right)\lambda^4 - \frac{1}{A_1}\left[D_{1r} - n^2\left(BD + \frac{3B_1 + B_{1r}}{2} - \frac{AP_1 - AP_{1r}}{4}\right)\right]\lambda^2 + \frac{1}{A_1}(-A_1 + AF_1 + BT_1)(n^4 - 2n^2) + \frac{1}{A_1}(AF_1 + BT) - \Omega_1^2 + \mathrm{FL}, \quad \lambda = k_{ns}R,$$

$$\Omega_1 = \Omega\sqrt{\frac{1 + (\rho_2 h_2)/(\rho_1 h_1)}{1 + (S_2 h_2)/(S_1 h_1)}},$$

$$\Omega = \sqrt{\rho_1 R^2 \omega^2 (1 - \mu_1^2)/E_1}, \quad X_{\text{pl}} = (1 - \mu_1^2)R^2 F_0/(E_1 h_1),$$
$$\mathrm{FL} = \Omega_1^2(\rho_f/\rho_1)(R/h_1)\mathrm{H}_n^{(2)}(k_s^r R)/((k_s^r R)\mathrm{H}_n^{(2)'}(k_s^r R)),$$
$$k_s^r = \pm\sqrt{(k_0)^2 - (k_{ns})^2}.$$

Let matrix **I** be the inverse of matrix **L**, then the spectral displacements can be obtained from Eq. (5) as follows:

$$\begin{bmatrix} \tilde{U}_{ns} & \tilde{V}_{ns} & \tilde{W}_{ns} \end{bmatrix}^{\mathrm{T}} = [I_{3\times 3}]\begin{bmatrix} 0 & 0 & X_{pl} \end{bmatrix}^{\mathrm{T}}, \tag{6}$$

$$\begin{bmatrix} \tilde{U}_{ns} & \tilde{V}_{ns} & \tilde{W}_{ns} \end{bmatrix}^{\mathrm{T}} = X_{pl}\begin{bmatrix} I_{13} & I_{23} & I_{33} \end{bmatrix}^{\mathrm{T}}, \tag{7}$$

where the elements of matrix $\mathbf{I}$ can be easily obtained from the elements of matrix $\mathbf{L}$ as

$$I_{13} = (L_{12}L_{23} - L_{13}L_{22})/(\det|\mathbf{L}|), \tag{8a}$$

$$I_{23} = (L_{12}L_{13} - L_{11}L_{32})/(\det|\mathbf{L}|), \tag{8b}$$

$$I_{33} = (L_{11}L_{22} - L_{12}L_{21})/(\det|\mathbf{L}|). \tag{8c}$$

Application of the inverse Fourier transform of Eqs. (8) give the shell displacements as

$$u(x) = \frac{1}{2\pi}\int_{-\infty}^{\infty} I_{13}X_{pl}\cos(n\theta)\exp(\mathrm{i}\omega t - \mathrm{i}k_{ns}x)\mathrm{d}(k_{ns}), \tag{9a}$$

$$v(x) = \frac{1}{2\pi}\int_{-\infty}^{\infty} I_{23}X_{pl}\sin(n\theta)\exp(\mathrm{i}\omega t - \mathrm{i}k_{ns}x)\mathrm{d}(k_{ns}), \tag{9b}$$

$$w(x) = \frac{1}{2\pi}\int_{-\infty}^{\infty} I_{33}X_{pl}\cos(n\theta)\exp(\mathrm{i}\omega t - \mathrm{i}k_{ns}x)\mathrm{d}(k_{ns}). \tag{9c}$$

3. Vibrational power flow analysis

3.1. Power flow input into the shell

When a harmonic external force $F(\theta, t)$ is applied to the shell wall radially, the radial response of the shell wall at $x = 0$ can be obtained from Eqs. (9). Thus, the input power flow from this driving force is shown as follows:

$$P_{\text{input}} = \int_0^{2\pi}\frac{1}{2}\,\mathrm{Re}\left[F_0\cos(n\theta)\frac{\partial w(0)^*}{\partial t}\right]R\,d\theta = \frac{\pi}{2\xi_n}\,\mathrm{Re}\{\mathrm{i}\omega F_0 w(0)^*\}, \tag{10}$$

where the asterisk denotes the complex conjugate, and

$$\xi_n = \begin{cases} 0.5, & n = 0, \\ 1, & n \neq 0. \end{cases} \tag{11}$$

The non-dimensional power flow is defined as

$$P'_{\text{input}} = \frac{P_{\text{input}}}{F_0^2\pi}\sqrt{\rho_1 E_1 R^2(1-\mu_1^2)}. \tag{12}$$

3.2. Power flow propagation along the shell axial direction

When an external harmonic line force is applied radially on the wall of the fluid-loaded viscoelastic shell, the forced vibration waves will propagate in the shell-fluid coupled system, and thus the power flow will also be transmitted along the shell axial direction. At the cross-section x, the shell displacements $u(x)$, $v(x)$, $w(x)$ and slope $\partial w(x)/\partial x$ can be obtained from Eqs. (9). Meanwhile, there will be four internal forces (moments) of the shell wall along the axial direction which can be easily derived from Flügge shell theory [18]. Then, the vibrational power flow transmitted by these forces (moments) can be expressed as

$$P_{N(x)} = \tfrac{1}{2}\int_0^{2\pi}\mathrm{Re}\left[N(x)(\mathrm{i}\omega)u(x)^*\right]R\,\mathrm{d}\theta, \tag{13a}$$

$$P_{T(x)} = \tfrac{1}{2}\int_0^{2\pi}\mathrm{Re}\left[T(x)(\mathrm{i}\omega)v(x)^*\right]R\,\mathrm{d}\theta, \tag{13b}$$

$$P_{S(x)} = \tfrac{1}{2}\int_0^{2\pi} \mathrm{Re}\left[S(x)(-\mathrm{i}\omega)w(x)^*\right] R\,\mathrm{d}\theta \tag{13c}$$

$$P_{M(x)} = \tfrac{1}{2}\int_0^{2\pi} \mathrm{Re}\left[M(x)(\mathrm{i}\omega)(\partial w(x)/\partial x)^*\right] R\,\mathrm{d}\theta. \tag{13d}$$

The total vibrational power flow in the shell wall is the sum of the component power flow carried by internal forces (moments) and expressed as

$$P_{\mathrm{shell}(x)} = P_{N(x)} + P_{T(x)} + P_{S(x)} + P_{M(x)}. \tag{14}$$

Once the external harmonic line force inputs power flow into the coupled system, the power flow in the shell transmitted along the axial direction can be known. According to symmetry, half of the input power will be transmitted in the positive direction of the shell axial while the other half will be transmitted in the opposite direction. Thus, the relative propagation power flow $P'_{\mathrm{shell}(x)} = P_{\mathrm{shell}(x)}/(0.5P_{\mathrm{input}})$ $(x>0)$ is defined to describe the characteristics of the power flow in the shell transmitted along the axial direction. In the same time, the ratios of the power flow carried by different shell internal forces (moments) (those are $P'_{N(x)} = P_{N(x)}/P_{\mathrm{shell}(x)}$, $P'_{T(x)} = P_{T(x)}/P_{\mathrm{shell}(x)}$, $P'_{S(x)} = P_{S(x)}/P_{\mathrm{shell}(x)}$ and $P'_{M(x)} = P_{M(x)}/P_{\mathrm{shell}(x)}$, respectively) to the total power in the shell wall also can be obtained.

4. Numerical computation and results discussion

The integrals in Eqs. (9) can be obtained by using a numerical integral method. This method is to integrate numerically along the pure imaginary axis of the complex wave number domain. Damping is introduced into the shell material by modifying the Young's modules E to be complex such as $E' = E(1+\mathrm{i}\eta)$. Thus, singularities in the integrand function along the integration path can be avoided and solution of free wave numbers of this system is unnecessary. Fuller [19] used this method to study the radiation of sound from an infinite elastic cylindrical shell excited by an internal monopole source. Xu and Zhang [20] used it to study the input energy flow into a shell filled with fluid.

For the infinite condition, the upper truncation point of the integral range has to be decided to obtain the results. In this paper, the value of integral in $[-b, b]$ is compared with that in $[-0.5b, 0.5b]$. If the difference is less than 1%, then b will be taken as the upper truncation point. When the integral range is decided, it is divided into many small integral ranges and the Gauss integral method is used in each integral range. This method is found to provide sufficient accuracy on the final results.

The following parameters of the coupled system have been used in the computations. $E_1 = 1.92\times 10^{11}(1-\mathrm{i}\eta_1)\ \mathrm{N/m^2}$, $\eta_1 = 0.02$, $\rho_1 = 7800\ \mathrm{kg/m^3}$, $\mu_1 = 0.3$, the parameters of the discussed viscoelastic material change with vibratory frequency and can be expressed as $E_2 = 3.0307\times 10^6 f^{0.625}(1+\mathrm{i}\eta_2)\ \mathrm{N/m^2}$ and $\eta_2 = 1.6274 f^{-0.072}$, $\rho_2 = 1100\ \mathrm{kg/m^3}$, $\mu_2 = 0.4$, $h_1 = h_2 = 0.02R$, $\rho_f = 1000\ \mathrm{kg/m^3}$, $c_f = 1500\ \mathrm{m/s}$. The magnitude of radial harmonic line force is supposed to be $F = 1\ \mathrm{N}$.

4.1. Power flow input into the shell

The non-dimensional input power flow P'_{input} against the non-dimensional driving frequency Ω for viscoelastic shell of different circumferential mode order n is plotted in Fig. 2. In order to investigate the influence of viscoelastic layer, the results of elastic shell are also plotted. As shown in the graphs, the input power flow varies with circumferential mode order and non-dimensional frequency. Resonance hump, at least one, will be shown on the input power flow curve for both elastic shell and viscoelastic shell in the frequency band of interest. As an additional mass, the viscoelastic layer will greatly influence the input power flow. Compared with the results of elastic shell, the stiffness of viscoelastic shell is increased, so the input power flow of viscoelastic shell becomes gentler and its amplitude declines. It indicates viscoelastic layer will restrict inputting power flow into the shell. With the increasing of the circumferential mode order, the vibration of the shell will present a more complex state and the reduced amplitude of resonance hump is further enlarged. Therefore, a conclusion can be drawn that the viscoelastic

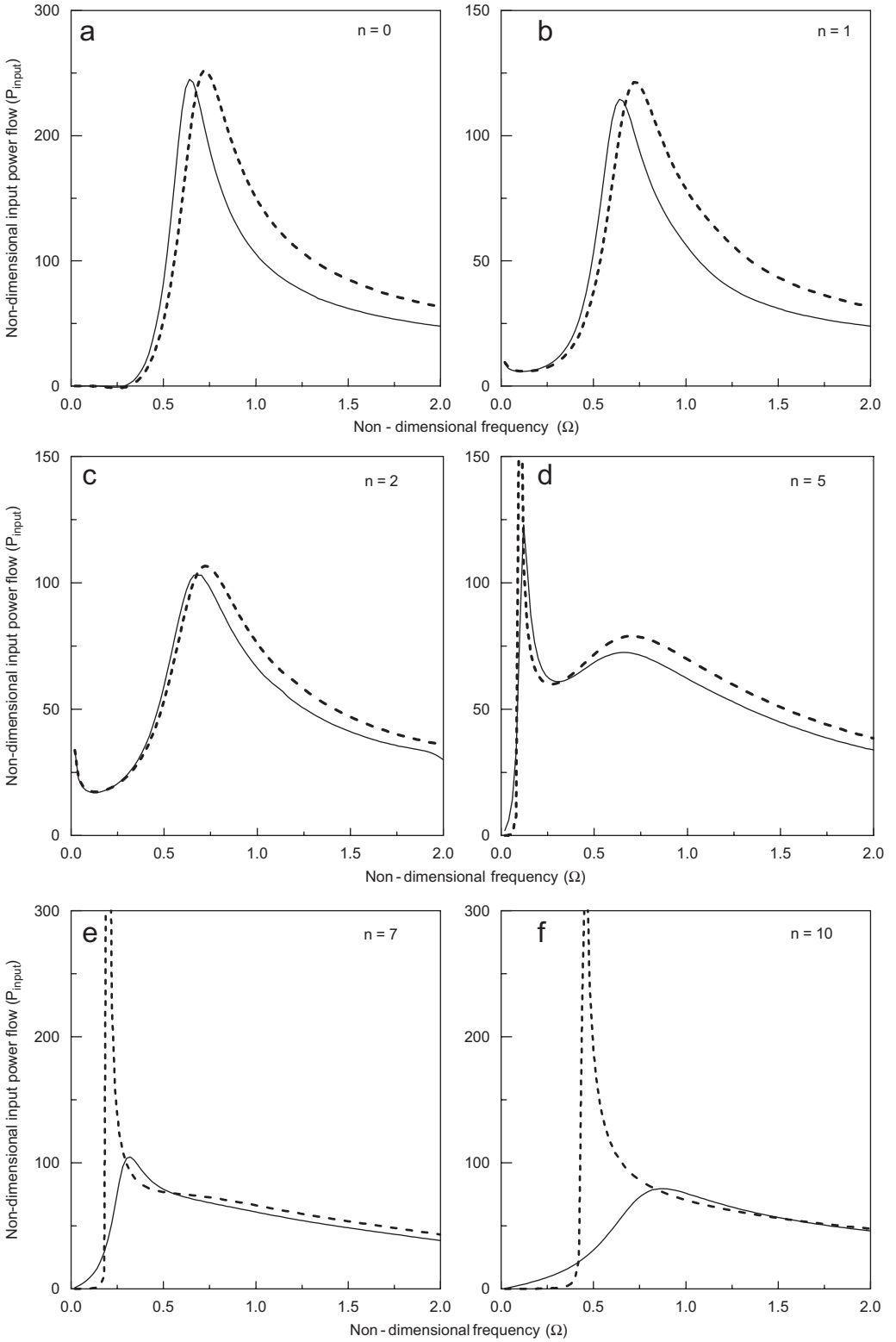

Fig. 2. Non-dimensional input power flow into a shell of different circumferential mode order *n*. - - - - elastic shell, —— viscoelastic shell.

layer can restrict the exciting force inputting power flow into the shell effectively when the circumferential mode order is high. For elastic shell, there exist so-called cut-off frequencies for some circumferential mode order. At those frequencies, the exciting force cannot input power flow into the structure [20]. But for viscoelastic shell, cut-off frequencies do not appear due to the influence of viscoelastic damping. This implies the exciting force can input power flow into the shell at any frequency and for any circumferential mode order.

Besides, it can be found that the effects of the damping are not so apparent at low frequencies for all circumferential mode order. With the increasing frequency, the effects of damping on restricting the input power flow become effective.

4.2. Influence of the damping layer thickness on the input power flow

The influences of the damping layer thickness on the input power flow for circumferential mode order $n = 2$ and 5 are given in Fig. 3. As shown in the drawings, the input power flow is reduced as the damping layer thickness increased from $h_2 = h_1$ to $h_2 = 1.5h_1$. Considered the influence of mode order, the resonance hump is crippled obviously especially for a higher circumferential mode order. It implies viscoelastic layer will play a more important role when the circumferential mode order is higher. But beyond resonance frequency, the effects of damping are limited. So once the external load is given in practice, it can be concluded viscoelastic damping will be more effective in restraining structure resonance and a thicker damping layer will be very helpful.

4.3. Power flow propagation along the shell axial direction

The relative propagation power flow $P'_{\mathrm{shell}(x)}$, $P'_{N(x)}$, $P'_{T(x)}$, $P'_{S(x)}$ and $P'_{M(x)}$ against the non-dimensional axial distance x/R are studied in Fig. 4. The analyses are focused on three typical frequencies (those are low frequencies $\Omega = 0.3$, middle frequencies $\Omega = 1.2$ and high frequencies $\Omega = 5.0$, respectively.) for circumferential mode order $n = 5$. In the drawings, negative value denotes power flow may be transmitted

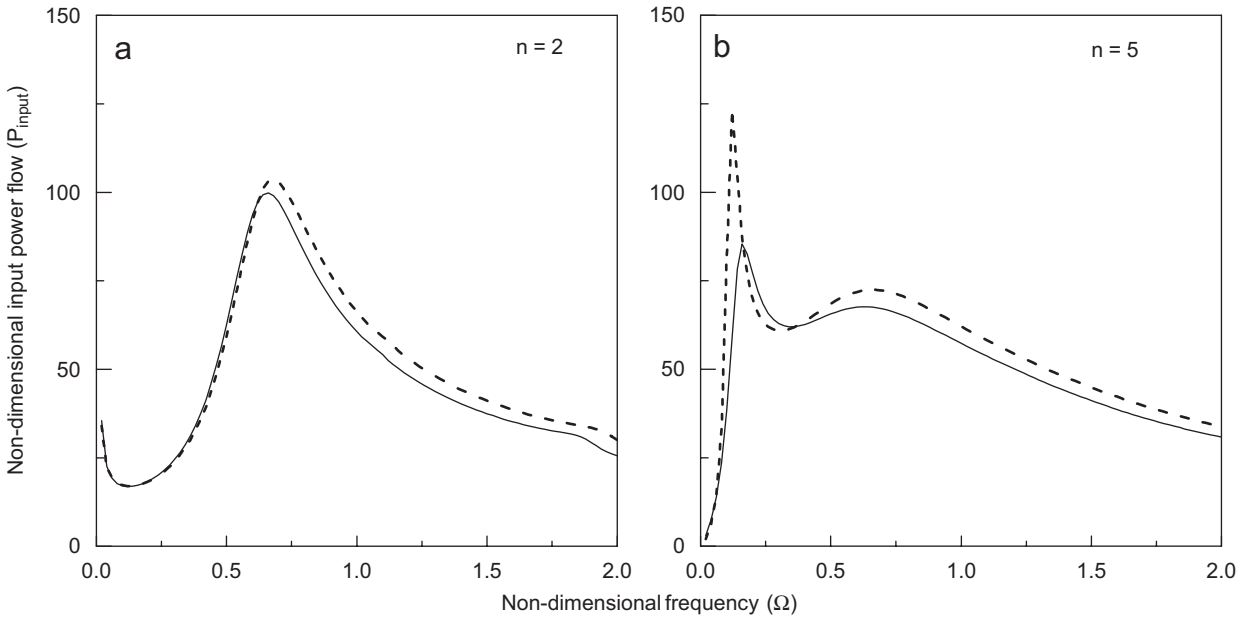

Fig. 3. Influence of the damping layer thickness on the input power flow ---- $h_2 = h_1$, —— $h_2 = 1.5h_1$.

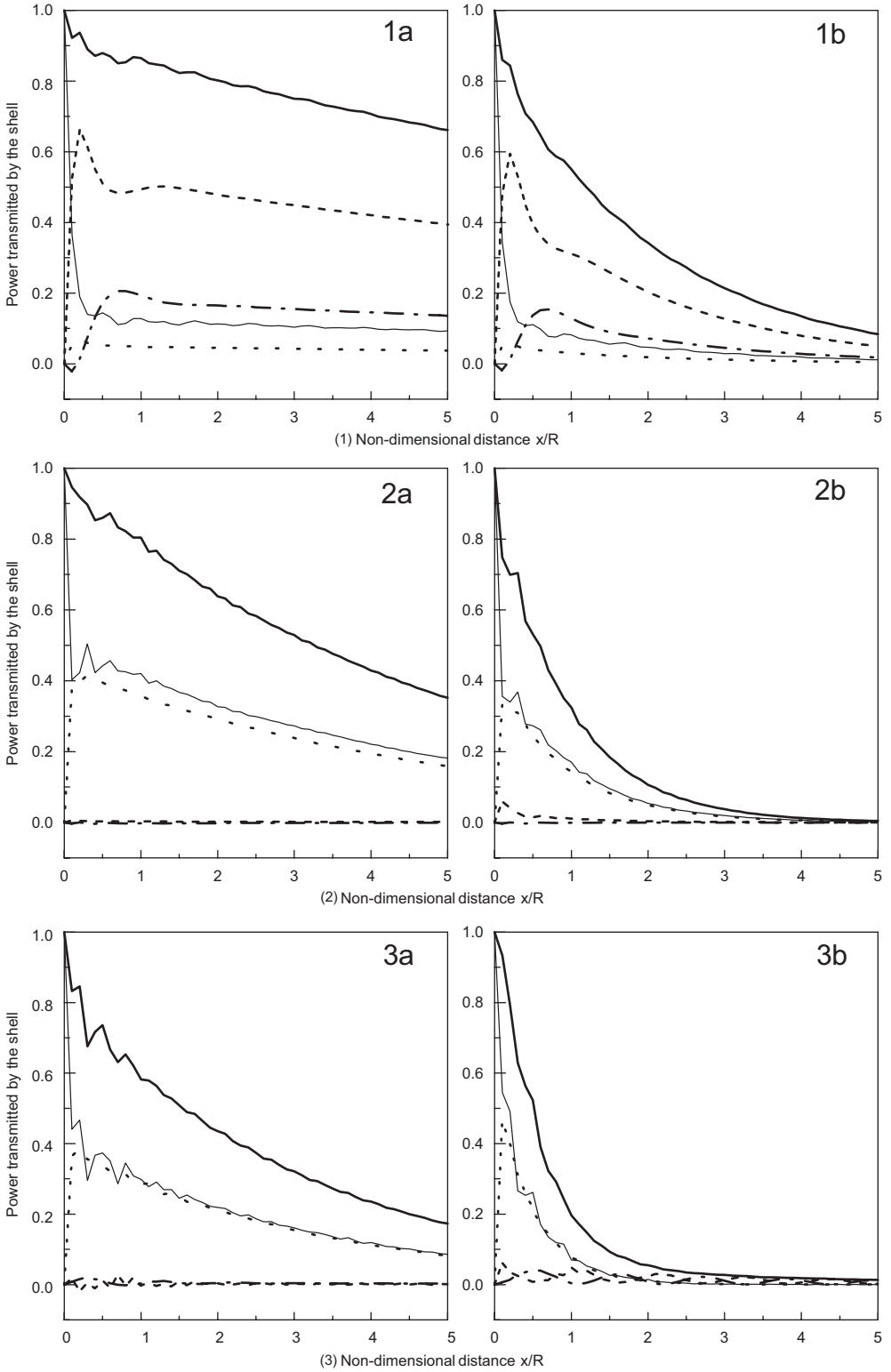

Fig. 4. Power transmitted by the shell for $5 = n$. (1a), (2a), (3a) elastic shell, (1b), (2b), (3b) viscoelastic shell. (1) $\Omega = 0.3$, (2) $\Omega = 1.2$, (3) $\Omega = 5.0$. ——— $P'_{\text{shell}(x)}$, —·—·—·— $P'_{N(x)}$, - - - - - $P'_{T(x)}$, ——— $P'_{S(x)}$, ... $P'_{M(x)}$.

in opposite direction. In order to investigate the influence of viscoelastic layer, the results of an elastic shell are also plotted.

As shown in the graphs, the characteristics of the propagation power flow of viscoelastic shell are similar to those of elastic shell. At the driving point, $x/R = 0$, there is $P'_{\text{shell}(x)} = 1$ for any circumferential mode order n and non-dimensional frequency Ω. At close range of the driving point, $P'_{\text{shell}(x)} \approx P'_{S(x)}$, the total energy is almost concentrated on flexural motion. When x/R increases, $P'_{\text{shell}(x)}$ will couple with the fluid and gradually attenuates because of damping and sound radiation.

At low frequencies ($\Omega = 0.3$, as shown in Fig. 4(1)), $P'_{S(x)} + P'_{M(x)} \ll P'_{N(x)} + P'_{T(x)}$, the power flow in the shell is mainly carried by axial force and torsional shear force. At middle or high frequencies (as shown in Figs. 4(2) and 4(3)), $P'_{S(x)} + P'_{M(x)} \gg P'_{N(x)} + P'_{T(x)}$, the motion of the shell wall is mainly in radial direction and the power flow in the shell is mainly carried by transverse shear force and bending moment. For all frequencies Ω and circumferential mode orders n, $P'_{S(x)} \approx P'_{M(x)}$, which means the power transmitted by the transverse shear force equals that transmitted by the bending moments. Due to the energy dissipation of damping and sound radiation, propagation power flow, $P'_{\text{shell}(x)}$, is attenuated along the shell axial direction. The decay speed of viscoelastic shell is much quicker than that of elastic shell, and the power is almost exhausted at $x/R = 5$.

Compared with the nearly linear attenuation mode of elastic shell, the attenuation of viscoelastic shell is exhibited in exponential form. So the propagation power flow will quickly be attenuated at middle or high frequencies due to viscoelastic damping. Considering the previous discussions about the input power flow in viscoelastic shell, a conclusion can be drawn that viscoelastic damping layer will have a good energy attenuation effect at middle or high frequencies.

5. Conclusions

By using wave propagation approach, the characteristics of the vibrational power flow in an infinite submerged unconstrained viscoelastic cylindrical shell are studied analytically. Several typical numerical computations are implemented and some comparisons are made with those of elastic shell.

The input power flow varies with circumferential mode order and frequency, and the viscoelastic damping layer will restrict the exciting force input power flow into the shell especially for a thicker damping layer and a higher circumferential mode order. Cut-off frequencies do not exist in viscoelastic shell so that the exciting force can input power flow into the shell at any frequency and for any circumferential mode order.

According to the symmetry propagation of power flow, at the driving point, $x/R = 0$, there is $P_{\text{shell}(x)} = 0.5P_{\text{input}}$ for any circumferential mode order n and non-dimensional frequency Ω. When non-dimensional axial distance x/R increases, $P'_{\text{shell}(x)}$ will couple with the fluid and gradually attenuates because of damping and sound radiation.

Considered the power flow transmitted by different internal forces (moments) of the shell wall, it can be found the power flow is mainly carried by axial force and torsional shear force at low frequencies while it is mainly carried by transverse shear force and bending moment at middle or high frequencies.

Relative to the nearly linear attenuation form of propagation power flow in elastic shell, propagation power flow in viscoelastic shell is exhibited in exponential attenuation form. Viscoelastic damping layer will have a good energy attenuation effect especially at middle or high frequencies.

Acknowledgements

The authors are grateful for the financial assistance provided by the National Natural Science Foundation of China (Contract no. 50375059).

Appendix A

$$A_1 = 1 + EB, \quad E = S_2/S_1, \quad S_1 = E_1/(1-\mu_1^2), \quad S_2 = E_2/(1-\mu_2^2),$$
$$E_2 = E_2^*(1+\mathrm{i}\eta_2), \quad B = h_2/h_1, \quad AF_1 = 1/G_{11} + EB/G_{22}, \quad G_{11} = 1 + d_1 h - \tfrac{1}{2}h,$$
$$G_{22} = 1 + d_1 h - \tfrac{1}{2}Bh, \quad h = h_1/R, \quad d_1 = d/h_1 = \frac{1}{2}\frac{1-E^*B^2}{1+E^*B}, \quad E^* = S_2^*/S_1,$$
$$S_2^* = E_2^*/(1-\mu_2^2), \quad AF_{1r} = \mu_1/G_{11} + EB\mu_2/G_{22},$$
$$BT_1 = \frac{h^2}{12}\left[(1/G_{11})^3 + E(B/G_{22})^3\right], \quad D = E_1 h_1/\left(1-\mu_1^2\right),$$
$$m = (\rho_1 h_1 + \rho_2 h_2), \quad A_{1r} = \mu_1(1+EBv), \quad v = \mu_2/\mu_1,$$
$$D_{1r} = h\mu_1\left[\tfrac{1}{3}(1-EB^2v) - 2d_1(1+EBv)\right],$$
$$B_1 = h^2\left[\tfrac{1}{3}(1+EB^3) - d_1(1-EB^2) + d_1^2(1+EB)\right],$$
$$BT_{1r} = \frac{h^2}{12}\left[\mu_1(1/G_{11})^3 + E\mu_2(B/G_{22})^3\right],$$
$$BD = \tfrac{1}{4}D_{1r} - \tfrac{1}{2}(A_1 - A_{1r}) + \tfrac{1}{2}(AF_1 - AF_{1r}) + \tfrac{1}{2}(BT_1 - BT_{1r}),$$
$$AQ = \tfrac{3}{4}D_{1r} + \tfrac{1}{2}(A_1 - A_{1r}) + \tfrac{3}{2}(B_1 - B_{1r}) - \tfrac{1}{4}(AP_1 - AP_{1r}),$$
$$B_{1r} = h^2\mu_1\left[\tfrac{1}{3}(1+EB^3v) - d_1(1-EB^2v) + d_1^2(1+EBv)\right],$$
$$AP_1 = h^3\left[(1-EB^4) - 4d_1(1+EB^3) + 6d_1^2(1-EB^2) - 4d_1^3(1+EB)\right],$$
$$AP_{1r} = h^3\mu_1\left[(1-EB^4v) - 4d_1(1+EB^3v) + 6d_1^2(1-EB^2v) - 4d_1^3(1+EBv)\right].$$

References

[1] Y. Kagawa, A. Krokstad, On the damping of cylindrical shells coated with viscoelastic materials, *ASME Publication* 69–Vibr (1969) 1–9.

[2] Š. Markuš, Damping properties of layered cylindrical shells vibration in axially symmetric modes, *Journal of Sound and Vibration* 48 (4) (1976) 511–524.

[3] Š. Markuš, Refined theory of damped axisymmetic vibrations of double-layered cylindrical shells, *Journal of Mechanical Engineering Science* 21 (1) (1979) 33–37.

[4] D.J. Mead, Š. Markuš, The forced vibration of a three-layer, damped sandwich beam with arbitrary boundary conditions, *Journal of Sound and Vibration* 10 (1969) 63–75.

[5] K.M. Iyer, Modal response of a circular cylindrical shell with damping layers, The Ohio State University, Ph.D. Thesis, 1980.

[6] A. Naiyar, N.T. Asnani, Damped axisymmetric vibration of two layered cylindrical shells, *Strojnicky Casopis* 37 (4) (1986) 479–490.

[7] H. Saito, H. Yamaguchi, Vibration damping characteristics of a thin cylindrical shell stiffened with viscoelastic rings, *Ingenieur Archiv* 48 (5) (1979) 301–311.

[8] O. Simkova, Š. Markuš, Damped vibration of a simply supported two-layered half-cylindrical shell, *Strojnicky Casopis* 36 (4/5) (1985) 631–640.

[9] X.M. Zhang, Vibrational power flow in a cylindrical shell periodically coated with viscoelastic materials, *Journal of Vibration Engineering* 6 (1) (1993) 1–9 (in Chinese).

[10] L. Cheng, R. Lapointe, Vibration attenuation of panel structures by optimally shaped viscoelastic coating with added weight consideration, *Thin-walled structure* 21 (1995) 307–326.

[11] A. Lumsdaine, R.A. Scott, Shape optimization of unconstrained viscoelastic layers using continuum finite elements, *Journal of Sound and Vibration* 216 (1) (1998) 29–52.

[12] C.R. Fuller, The input mobility of an infinite circular cylindrical shell filled with fluid, *Journal of Sound and Vibration* 87 (1983) 409–427.

[13] M.B. Xu, W.H. Zhang, Vibrational power flow input and transmission in a circular cylindrical shell filled with fluid, *Journal of Sound and Vibration* 234 (2000) 387–403.

[14] S.V. Sorokin, J.B. Nielsen, N. Olhoff, Green's matrix and the boundary integral equation method for the analysis of vibration and energy flow in cylindrical shells with and without internal fluid loading, *Journal of Sound and Vibration* 273 (2004) 815–847.

[15] J. Yan, T.Y. Li, T.G. Liu, et al., Characteristics of the vibrational power flow propagation in a submerged periodic ring-stiffened cylindrical shell, *Applied Acoustics* 67 (2006) 550–569.
[16] X.M. Zhang, G.R. Liu, K.Y. Lam, Vibration analysis of thin cylindrical shells using wave propagation approach, *Journal of Sound and vibration* 239 (3) (2001) 397–403.
[17] P.M. Morse, K.U. Ingard, *Theoretical Acoustics*, McGraw-Hill, New York, 1968.
[18] W. Flügge, *Stress in Shells*, Spring, Berlin, New York, 1973.
[19] B.J. Brevart, C.R. Fuller, Energy exchange between the coupled media of impulsively excited fluid-filled elastic cylinders, *Journal of Sound and Vibration* 190 (1996) 763–774.
[20] M.B. Xu, X.M. Zhang, Vibration power flow in a fluid-filled cylindrical shell, *Journal of Sound and Vibration* 218 (1998) 587–598.